Supplementary material.

Figure S1. Colony morphology of wild-type and mutant *S. aureus* strains.

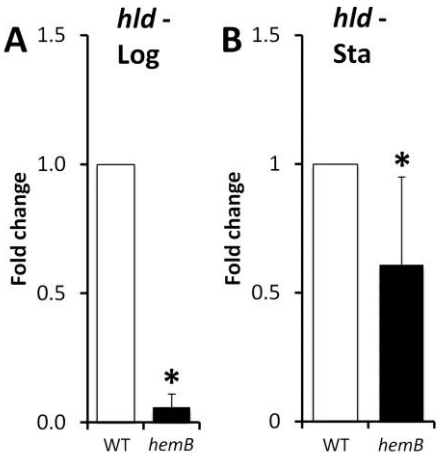

Figure S2. Levels of *hld* (RNAIII) transcript in logarithmic (Log) and stationary phase (Sta) are significantly reduced in a *hemB*::Tn mutant (*hemB*) relative to those seen in the wild-type (WT). Data represent the relative *hld* expression levels in wild-type and *hemB*::Tn *S. aureus* as derived from the mean average of two independent experiments done in triplicate. Error bars represent the standard deviation of the mean. Values for the *hemB*::Tn mutant were significantly lower than those of the wild-type in both growth phases (p = <0.05 by student's t-test).

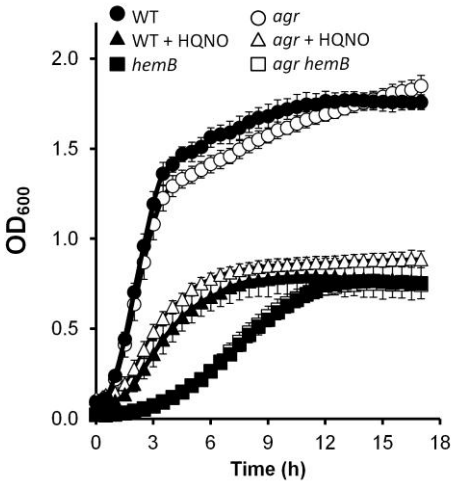

Figure S3. Expression of *gfp* from the P3 promoter does not adversely affect growth. Wild-type SH1000 (closed circles), *agr*-defective SH1001 (open circles) grown in TSB only or in the presence of HQNO (SH1000 closed triangles, SH1001 open triangles) were compared for growth rate and final density. Also shown is growth of *hemB*::Tn (open squares) and *hemB*::Tn *agr* (closed squares). Each data point represents the mean of 4 independent experiments done in triplicate. Error bars represent the standard deviation of the mean. Values for *agr*-competent strains were not significantly lower than those for *agr*-deficient strains at any time point.

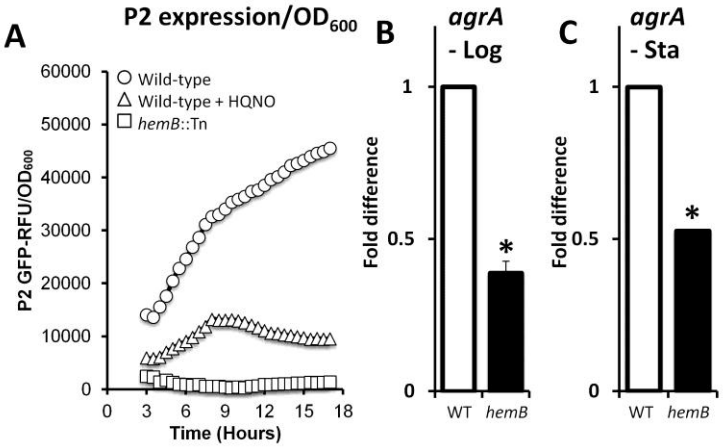

Figure S4. Expression of the RNAII transcript is similar to that of RNAIII in the absence and presence of a functional electron transport chain. P2 activity was determined and adjusted for growth (OD_{600}) as described for P3 for wild-type bacteria grown in the absence (circles) or presence (triangles) of HQNO (A). Values for the *hemB*::Tn mutant are represented by squares (A). These data were supported by RT-PCR analysis of *agrA* transcript levels in both logarithmic (log) and stationary (sta) phase cultures of wild-type (WT) and *hemB*::Tn (*hemB*) strains (B). Data in A represent the mean of 4 independent experiments done in triplicate. Error bars representing the standard deviation of the mean were omitted for clarity but were less than 10 % of the mean. Data in (B) are generated from two independent experiments done in triplicate. Values for the *hemB*::Tn mutant were significantly lower than those of the wild-type in both growth phases (p = <0.05 by student's t-test).

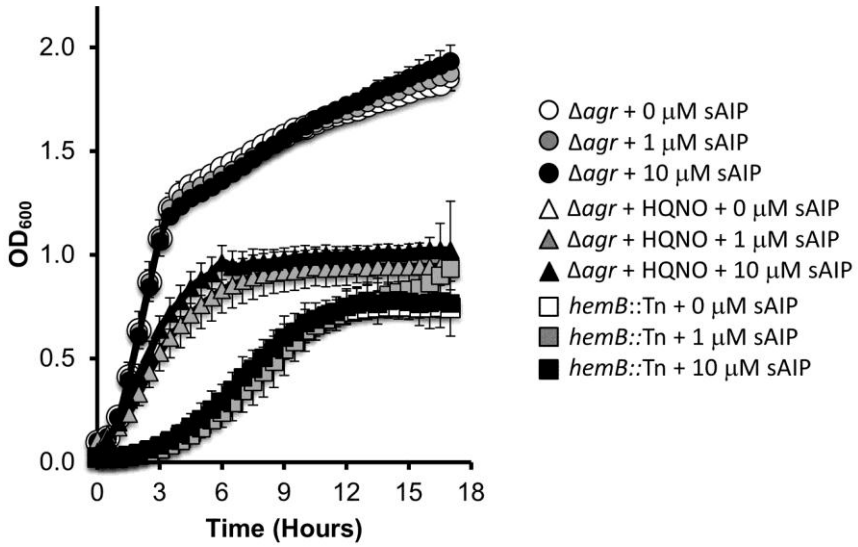

Figure S5. sAIP does not affect the growth of *agr*-defective strains. The growth (OD_{600}) of SH1001 (Δ*agr*) in the absence (circles) or presence (triangles) of HQNO, in the absence or presence of sAIP (0, 1 or 10 μM) was measured over time. Also shown is the growth of a *hemB*::Tn Δ*agr* strain (squares) in the presence of the same concentrations of sAIP. Each data point represents the mean of 4 independent experiments done in triplicate. Error bars represent the standard deviation of the mean. Values for growth in the absence of sAIP were not significantly different from those for strains grown in the presence of either concentration of sAIP at any time point.

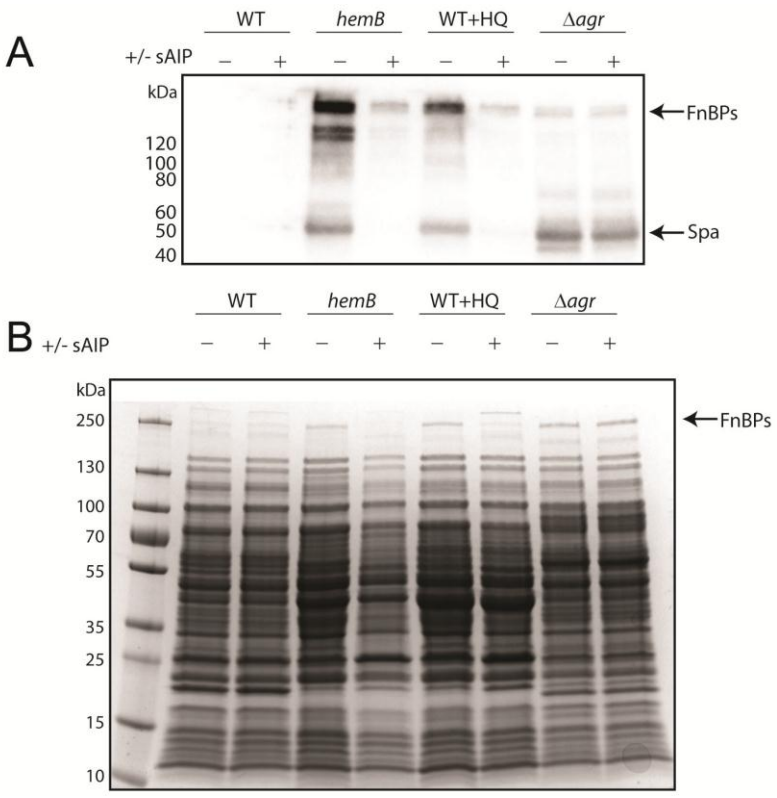

Figure S6. sAIP modulates expression of fibronectin binding proteins and protein A in both the absence and presence of a functional electron transport chain. (A) Total protein extracts from wild-type (WT) *S. aureus* SH1000, *hemB*::Tn or SH10001 (Δ*agr*) grown in the presence (+HQ) or absence of HQNO or sAIP (as indicated in figures) were subjected to blot overlay with human fibronectin to detect fibronectin binding proteins (FnBPs). Also visible in panel A are bands corresponding to the immunoglobulin-binding protein A (Spa). (B) Corresponding SDS-PAGE of protein extracts used in panel A. Visible are bands corresponding to FnBPs (indicated).